International Journal of Engineering

Ivestigation of Entropy Generation in 3-D Laminar Forced Convection Flow over a Backward Facing Step with Bleeding

M. Shamsi Kooshki[a], S. A. Gandjalikhan Nassab [a] *, A. B. Ansari[b]

[a] *Department of Mechanical Engineering, Shahid Bahonar University, kerman, Iran.*
[b] *Department of Mechanical Engineering, Tehran University, Tehran, Iran.*

P A P E R   I N F O

A B S T R A C T

A numerical investigation of entropy generation in laminar forced convection of gas flow over a backward facing step in a horizontal duct under bleeding condition is presented. For calculation of entropy generation from the second law of thermodynamics in a forced convection flow, the velocity and temperature distributions are primary needed. For this purpose, the three-dimensional Cartesian coordinate system is used to solve the Navier-Stokes and energy equations by the computational fluid dynamic techniques. Discretized forms of these equations are obtained by the finite volume method and solved using the SIMPLE algorithm. The numerical results are presented graphically and the effects of bleeding coefficient on the distributions of entropy generation and Nusselt numbers along the duct's wall and also on total entropy generation are presented. The numerical results can be used in design of such thermal system with high performance. Comparison of numerical results with the available data published in open literature shows a good consistency.

NOMENCLATURE

AR	Aspect ratio	**Greek Symbols**	
Be	Bejan number	α	thermal diffusivity (m^2/s)
Br	Brinkman number	κ	thermal conductivity
ER	expansion ratio	μ	dynamic viscosity ($N.s\,/\,m^2$)
h	upstream height of the duct	ν	kinematic viscosity ($m^2\,/\,s$)
H	downstream height of the duct	ρ	density ($kg\,/\,m^3$)
Ns	entropy generation number	τ	dimensionless temperature parameter
Pe	Peclet number	Θ	dimensionless temperature
Pr	Prandtl number	σ	bleeding coefficient
Re	Reynolds number	**Subscripts**	
s''_{gen}	volume rate of entropy generation	in	inlet section
T	temperature (K)	w	wall
U_0	average velocity of the incoming flow at the inlet section (m/s)	cond	conduction
X_i	Length of permeable segment of the bottom wall	visc	viscous
x, y, z	horizontal and vertical distance, respectively (m)	lw	bottom wall
X, Y, Z	dimensionless horizontal and vertical coordinate, respectively	uw	upper wall
x_r	reattachment length (m)		

* Corresponding Author Email: *ganj110@mail.uk.ac.ir* (S. A. Gandjalikhan Nassab)

1. INTRODUCTION

Forced convection flow in channels with abrupt contraction or expansion in flow geometry occurs in many engineering applications where heating or cooling process is required. Electronic cooling equipment, cooling of turbine blades and nuclear reactors, environmental control systems, combustion chambers and many other heat transfer devices are good examples of these applications. Mixing of high and low fluid energies occurs in recirculated flow regions and has great effects on the heat transfer performance of these devices. Therefore, studies on separated flows both theoretically and experimentally have been conducted extensively during the past decade.

Flow over backward-facing step (BFS) has the most features of separated flows. Although, the geometry of BFS flow is very simple, but the heat transfer and fluid flow over this type of step contain most of complexities. Consequently, it has been used in the benchmark investigations.

There are many experimental and numerical studies about laminar convection flow over BFS in a duct by several investigators. Armaly et al. [1] reported velocity measurements for three-dimensional laminar separated airflow adjacent to a BFS using the two-component laser Doppler velocimeter. The flow measurements covered a Reynolds number range between $98.5 \leq Re \leq 525$ and velocity distributions that were measured at different planes downstream from the step, were presented. Their results showed some interesting flow behaviors that could not be deduced from two-dimensional studies. Nie and Armaly [2] performed Laser-Doppler velocity measurements adjacent to the bounding walls of three-dimensional backward-facing step flow for the purpose of mapping the boundaries of reverse flow regions. It was shown that by increasing in Reynolds number, the size of reverse flow regions increases and moves further downstream in the laminar flow regime; decreases and moves upstream in the transitional flow regime; and remains almost constant or diminishes in the turbulent flow regime. Iwai et al. [3] numerically simulated three-dimensional laminar flows over a BFS in order to investigate the effects of duct aspect ratio on flow and heat transfer characteristics. Close attention was paid to the distribution patterns of both Nusselt number and the skin friction coefficient on the bottom wall. They found that an aspect ratio of as large as AR=16 at least was needed to obtain a 2-D region near the centerline at Re=250. Three-dimensional and incompressible laminar forced convection flow immediately after a BFS in a rectangular duct was studied by Nie et al. [4]. The effects of step height on the flow and heat transfer characteristics were investigated. It was found that the size of primary recirculation region and the maximum Nusselt number

increase as the step height increases. Nie and Armaly [5] studied distributions of the wall temperature, Nusselt number and friction coefficient on all of the bounding walls of laminar three-dimensional forced convection flow over a BFS in a rectangular duct. Local and average convection coefficients for a Reynolds number range of 150–450 were investigated and some results were compared with their equivalent from the two-dimensional case. A review of research on laminar convection flow over backward and forward facing step was done by Abu-Mulaweh [6]. In that study, a comprehensive review of such flows, those have been reported in several studies in the open literature was presented. The purpose was to give a detailed summery of the effect of several parameters such as step height, Reynolds number, Prandtl number and the buoyancy force on the flow and temperature distributions downstream of the step. Several correlation equations reported in many studies were also summarized.

Iwai et al. [7] investigated three-dimensional numerical mixed convection flow over a BFS in a rectangular duct. Effect of the inclination angle was the main objective in that investigation. It was found that this parameter has effects on fluid flow and heat transfer behaviors of convection system. Chen et al. [8] simulated a three-dimensional laminar forced convection adjacent to an inclined BFS to examine the effects of step inclination on flow and heat transfer distributions. It was shown that the downwash adjacent to the sidewall becomes stronger as the step inclination angle increases and the friction coefficient inside the primary recirculation region increases with increasing in step inclination angle.

Nie et al. [9] numerically simulated a three-dimensional laminar forced convection flow over a BFS in a rectangular duct to examine the effects of baffle on flow and heat transfer behavior of convective flow. A baffle was mounted on the upper wall and its distance from the BFS was varied. They showed that this baffle increases the value of maximum Nusselt number at the stepped wall.

One of the primary objectives in the design of any energy system is to conserve the useful energy in a certain process. The useful energy is destroyed by the irreversibility associated within the process components. It is clear that the irreversibility cannot be avoided completely because of the second law of thermodynamics, but it can be minimized in order to save the available energy. Entropy generation analysis provides a useful tool to identify the irreversibility in any thermal system as well as to determine the optimum condition for any process. Heat transfer and viscous dissipation are the only sources of entropy generation in force convection fluid flow.

Numerical studies on the entropy generation in convective heat transfer problems were carried out by

many investigators. Bejan [10-11] showed that entropy generation in convective fluid flow is due to heat transfer and viscous shear stresses. A numerical solution procedure for predicting local entropy generation for a fluid impinging on a heated wall was developed by Drost and White [12]. Abu-nada [13-15] analyzed the convection flow over a BFS in a duct to investigate the amount of entropy generation in this type of flow. In that work, the set of governing equations were solved by the finite volume method and the distributions of entropy generation number, friction coefficient and Nusselt number on the duct walls were calculated. Moreover, the effects of blowing and suction on the entropy generation number and Bejan number were presented. In a recent study, Bahrami and Gandjalikhan Nassab [16] analyzed the convection flow over forward facing step in a duct to investigate the amount of entropy generation in this type of flow. A numerical investigation of entropy generation in laminar forced convection of gas flow over a recess including two inclined backward and forward facing steps in a horizontal duct was studied by Atashafrooz et al. [17]. In that study, the effects of step inclination angle, recess length and Reynolds number on the distributions of entropy generation number and Bejan number and also on total entropy generation were investigated.

Although there are many studies about entropy generation in many process components such as BFS flows, but a careful inspection of literature shows that the entropy generation in three-dimensional convection flow over a BFS under bleeding condition on the bottom wall, is still not studied. Therefore, the present research deals to the calculation of entropy generation in a forced convection flow adjacent to BFS in a 3-D horizontal duct with emphasis on the effect of bleeding coefficient. Toward this end, the set of governing equations those are conservations of mass, momentum and energy along with the entropy generation equations are solved by the computational fluid dynamics (CFD) technique in the Cartesian coordinate system.

2. PROBLEM DESCRIPTION

Three-dimensional laminar forced convection flow adjacent to BFS in a horizontal heated rectangular duct under bleeding condition on the bottom wall is numerically simulated. The computational domain is schematically illustrated in Figure 1. The upstream and downstream heights of the duct are h and H, respectively. The aspect ratio AR=D/H of the duct is equal to 4 and the expansion ratio ER=H/h is considered equal to 2 in the present computations. The upstream length of the duct is considered to be L_1=2H and the downstream length of the duct is L_2=25H. This is made to ensure that the flow at the inlet section of the duct is
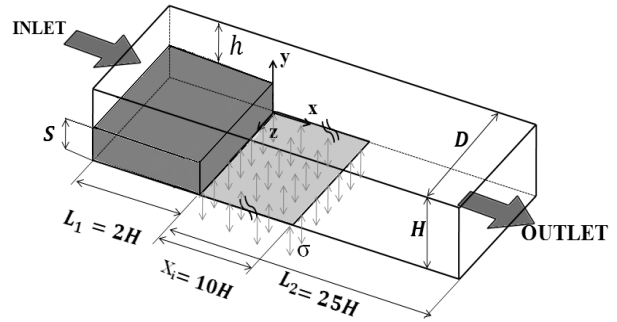

Figure 1. Sketch of problem geometry

not affected significantly by the sudden expansion in the geometry at the step and the flow at the exit section becomes fully developed. Part of the channel's bottom wall, adjacent to the step, is considered permeable (see Figure 1). In this figure, X_i represents the length of permeable segment of the bottom wall, which is considered to be X_i=10H. The arrows that are shown on the permeable segment represent the direction of mass bleed through the wall. Inward direction represents blowing in the domain and outward direction represents suction flow out of the domain.

3. BASIC EQUATIONS

For incompressible, steady, and three dimensional laminar forced convection flow, the governing differential equations are the conservations of mass, momentum, and energy that can be written as follows:

$$\frac{\partial u}{\partial x} + \frac{\partial v}{\partial y} + \frac{\partial w}{\partial z} = 0 \tag{1}$$

$$u\frac{\partial u}{\partial x} + v\frac{\partial u}{\partial y} + w\frac{\partial u}{\partial z} = -\frac{1}{\rho}\frac{\partial p}{\partial x} + \nu\left(\frac{\partial^2 u}{\partial x^2} + \frac{\partial^2 u}{\partial y^2} + \frac{\partial^2 u}{\partial z^2}\right) \tag{2}$$

$$u\frac{\partial v}{\partial x} + v\frac{\partial v}{\partial y} + w\frac{\partial v}{\partial z} = -\frac{1}{\rho}\frac{\partial p}{\partial y} + \nu\left(\frac{\partial^2 v}{\partial x^2} + \frac{\partial^2 v}{\partial y^2} + \frac{\partial^2 v}{\partial z^2}\right) \tag{3}$$

$$u\frac{\partial w}{\partial x} + v\frac{\partial w}{\partial y} + w\frac{\partial w}{\partial z} = -\frac{1}{\rho}\frac{\partial p}{\partial z} + \nu\left(\frac{\partial^2 w}{\partial x^2} + \frac{\partial^2 w}{\partial y^2} + \frac{\partial^2 w}{\partial z^2}\right) \tag{4}$$

$$\frac{\partial}{\partial x}(uT) + \frac{\partial}{\partial y}(vT) + \frac{\partial}{\partial z}(wT) = \alpha\left(\frac{\partial^2 T}{\partial x^2} + \frac{\partial^2 T}{\partial y^2} + \frac{\partial^2 T}{\partial z^2}\right) \tag{5}$$

In these equations, u, v and w are the velocity components in x-, y- and z-directions, respectively, P the pressure, T the temperature, ν the kinematic viscosity and α is the thermal diffusivity.

The boundary conditions are treated as no slip conditions at the solid walls (zero velocity) and constant temperature of T_w for all boundary walls. At the inlet duct section, the gas flows with uniform velocity and also uniform temperature of T_{in}, which is assumed to be

lower than T_w. Uniform velocity of v_w is allowed to bleed through the porous bottom wall. At the outlet section, zero axial gradients for velocity components and gas temperature are employed.

3. 1. Non-dimensional Forms of the Governing Equations

In numerical solution of the set of governing equations, the following dimensionless parameters are used to obtain the non-dimensional forms of these equations:

$$(X, Y, Z) = (\frac{x}{H}, \frac{y}{H}, \frac{z}{H}), \quad (U,V,W) = (\frac{u}{U_\circ}, \frac{v}{U_\circ}, \frac{w}{U_\circ}), \quad v_w^* = \frac{v_w}{U_\circ},$$

$$P = \frac{p}{\rho U_\circ^2}, \quad \sigma = \frac{v_w}{U_\circ}, \quad \Theta = \frac{T - T_{in}}{T_w - T_{in}}, \quad Pr = \frac{v}{\alpha}, \quad Re = \frac{\rho U_o H}{\mu},$$

$$Pe = Re.Pr$$

Using the above parameters, the non-dimensional forms of the governing equations become as follows:

$$\frac{\partial U}{\partial X} + \frac{\partial V}{\partial Y} + \frac{\partial W}{\partial Z} = 0 \tag{6}$$

$$\frac{\partial}{\partial X}\left(U^2 - \frac{1}{Re}\frac{\partial U}{\partial X}\right) + \frac{\partial}{\partial Y}\left(UV - \frac{1}{Re}\frac{\partial U}{\partial Y}\right) + \frac{\partial}{\partial Z}\left(UW - \frac{1}{Re}\frac{\partial U}{\partial Z}\right)$$
$$= -\frac{\partial P}{\partial X} \tag{7}$$

$$\frac{\partial}{\partial X}\left(UV - \frac{1}{Re}\frac{\partial V}{\partial X}\right) + \frac{\partial}{\partial Y}\left(V^2 - \frac{1}{Re}\frac{\partial V}{\partial Y}\right) + \frac{\partial}{\partial Z}\left(VW - \frac{1}{Re}\frac{\partial V}{\partial Z}\right)$$
$$= -\frac{\partial P}{\partial Y} \tag{8}$$

$$\frac{\partial}{\partial X}\left(UW - \frac{1}{Re}\frac{\partial W}{\partial X}\right) + \frac{\partial}{\partial Y}\left(VW - \frac{1}{Re}\frac{\partial W}{\partial Y}\right) + \frac{\partial}{\partial Z}\left(W^2 - \frac{1}{Re}\frac{\partial W}{\partial Z}\right)$$
$$= -\frac{\partial P}{\partial Z} \tag{9}$$

$$\frac{\partial}{\partial X}\left(U\theta - \frac{1}{Pe}\frac{\partial \theta}{\partial X}\right) + \frac{\partial}{\partial Y}\left(V\theta - \frac{1}{Pe}\frac{\partial \theta}{\partial Y}\right) + \frac{\partial}{\partial Z}\left(W\theta - \frac{1}{Pe}\frac{\partial \theta}{\partial Z}\right) = 0 \tag{10}$$

The values of bleeding coefficient used in the present work are $\pm$ (0, 0.005, and 0.01), where positive values correspond to blowing and negative values correspond to suction. The case of zero value of bleeding coefficient corresponds to impermeable wall. Therefore, the non-dimensional velocity at the porous section is equal to the bleeding coefficient which is expressed as:

$$\sigma = v_w^* \tag{11}$$

3. 2. Entropy Generation Equations

In the present study, one of the physical quantities of interest is the rate of entropy generation inside the flow domain. For calculating this parameter, the following dimensionless quantities are defined:

$$Ns = \frac{s_{gen}'' D_h^2}{\kappa \tau^2}, \quad \tau = \frac{T_w - T_{in}}{T_{in}}, \quad Br = \frac{\mu U_0^2}{\kappa (T_w - T_{in})},$$
$$\Psi = \frac{Br}{\tau} \tag{12}$$

In the above equations, Ns is the entropy generation number, s_{gen}'', the volume rate of entropy generation, Br the Brinkman number and τ is the non-dimensional temperature parameter. Using the above parameters, the entropy generation in dimensionless form can be expressed as [20]

$$Ns = \left[\left(\frac{\partial \Theta}{\partial X}\right)^2 + \left(\frac{\partial \Theta}{\partial Y}\right)^2 + \left(\frac{\partial \Theta}{\partial Z}\right)^2\right] + \tag{13}$$

$$\Psi\left\{2\times\left[\left(\frac{\partial U}{\partial X}\right)^2 + \left(\frac{\partial V}{\partial Y}\right)^2 + \left(\frac{\partial W}{\partial Z}\right)^2\right] + \left[\left(\frac{\partial U}{\partial Y}\right) + \left(\frac{\partial V}{\partial X}\right)\right]^2 \\ + \left[\left(\frac{\partial U}{\partial Z}\right) + \left(\frac{\partial W}{\partial X}\right)\right]^2 + \left[\left(\frac{\partial V}{\partial Z}\right) + \left(\frac{\partial W}{\partial Y}\right)\right]^2\right\}$$

This equation is used to solve for the entropy generation number at each grid point in the flow domain. Equation (13) contains two parts. The first term represents entropy generation due to the heat transfer (Ns_{cond}), while the second term represents the entropy generation due to the fluid viscous effect (Ns_{visc}). In addition, the Bejan number which is the ratio of entropy generation due to conduction to the total entropy generation can be expressed as follow:

$$Be = \frac{Ns_{cond}}{Ns_{cond} + Ns_{visc}} \tag{14}$$

According to the definition of Bejan number, the irreversibilities due to the viscous effect are dominant when $Be \leq 1/2$. When $Be \geq 1/2$, the heat transfer irreversibilities dominate the process and if Be=0.5, the entropy generation due to the viscous effect and heat transfer are equal.

In addition, the total entropy generation which shows the amount of irreversibility due to both viscous friction and heat transfer factors can be expressed as:

$$Ns = \int_\forall Ns(X, Y, Z)d \forall \tag{15}$$

where, $\forall$ is the volume of flow domain.

4. NUMERICAL PROCEDURE

In numerical solution of the Navier-Stokes and energy equations, Equations (6)–(10), discretized forms of these equations were obtained by integrating over an element cell volume. The staggered type of control volume for the x-, y- and z- velocity components was used, while the other variables of interest were computed at the grid nodes. Discretized forms of the governing equations were numerically solved by the SIMPLE algorithm of Patankar and Spalding [18]. Numerical solutions were obtained iteratively by the line-by-line method. Numerical calculations were performed by writing a computer program in FORTRAN.

As the result of grid tests for obtaining the grid-independent solutions, extensive mesh testing was performed in Table 1, for a convection step flow at Re=250 with aspect ratio AR=4 and expansion ratio ER=2. The grid is concentrated close to the duct walls and near to the step corners, in order to ensure the accuracy of the numerical solution. For this test case, the averaged value of Nu on the bottom wall in z-direction is calculated and the maximum value of this parameter along the flow direction for different grid sizes is recorded in Table 1. As it is shown in this table, a grid size of 521×36×36 can be chosen for obtaining the grid independent solution, such that the subsequent numerical calculations are made based on this grid size. The convergence criterion was assumed to have been achieved when the values of residual terms in the momentum and energy equations did not exceed 10^{-4}.

5. VALIDATION OF COMPUTATIONAL RESULTS

To validate the present numerical results, the reattachment length on the bottom wall for a three-dimensional fluid flow over a BFS is compared with that presented by Li [19]. The results are plotted in Figure 2. The maximum reattachment length occurs at the sidewall and not at the mid-plane, as one would expect. The computed reattachment point in the case of ER=2 is composed with experiment in Figure 2, where a good consistency is seen between theoretical and experimental results. Moreover, for validation of numerical results about heat transfer behavior of convection flow, the distribution of Nusselt number along the centerline on the bottom wall, in the case of ER=2 and AR=4, is compared with the results of Iwai et al. [3] in which a forced convection flow of gas over a BFS was investigated. The results are presented graphically in Figure 3. In this test case, the inlet flow was assumed to be hydro-dynamically steady and fully developed. Other velocity components V and W were set to zero at the inlet, while the fluid was assumed to have a uniform temperature at this section. The side walls were treated adiabatic, while the other walls were kept at constant temperature higher than the inlet fluid temperature. Figure 3 illustrates that after the backward step, Nu number increases and reaches to a maximum value that is occurs near to the reattachment point after which, Nu decreases until it approaches to a fixed value far from the step. However, Figure 3 shows a good consistency between the present numerical results with those reported in some references [3].

Since, there is not any theoretical result about entropy generation in three-dimensional forced convection flow adjacent to a backward facing step, the present numerical implementation was validated by reproducing the results of Abu-Nada [15] in which a

forced convection gas flow over a BFS takes place in two dimensional condition. In this test case, the temperature of the top wall was lower than the temperature of the bottom wall. The gas temperature profile at the inlet section was also assumed to be fully developed.

TABLE 1. Grid independence study

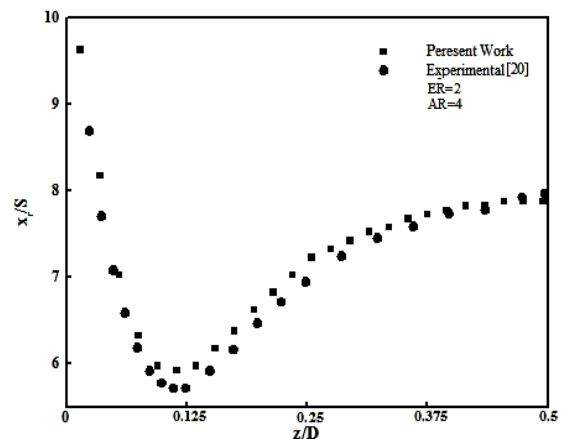| Grid size	Nu_{max}
10×10×135	2.60428
20×20×270	2.82022
24×24×324	2.89688
30×30×405	2.98373
36×36×521	3.04929
40×40×536	3.04935
44×44×566	3.04939

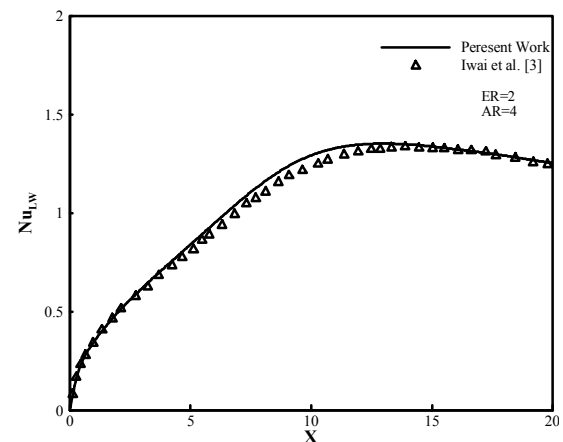**Figure 2.** Span wise distribution of the reattachment length and comparison with experiment

Figure 3. Nu distribution on the bottom wall in the mid-plane (Re =500).

Moreover, the bottom wall was permeable with bleeding condition including both suction and blowing. Variation of entropy generation along the bottom wall is compared with that obtained by Abu-Nada [15] in the case of ER=2, Re=400 and σ =-0.005. The results are presented in Figure 4. This figure shows that the minimum value of entropy generation occurs exactly at the bottom step corner, where the fluid has no motion. Furthermore, this figure indicates that the maximum value of *Ns* occurs inside the recirculation zone and then drops sharply to a very low value at the reattachment point. Then *Ns* increases and approaches to a fixed value far from the step. However, a good consistency exists between the present numerical results with those reported by Abu-Nada [15].

6. RESULTS AND DISCUSSIONS

The present results are about three-dimensional incompressible laminar forced convection flow immediately after the backward step in a rectangular duct at Reynolds number equal to 250, aspect ratio of AR=4 with considering the bleeding conditions. In addition, the Prandtl number is kept constant at 0.71 to guarantee constant fluid physical properties for moderate and small values of temperature difference (T_w-T_{in}). It is worth mentioning that the values of bleed coefficient used in the present work are $\pm$ (0, 0.005, and 0.01), where positive and negative values correspond to blowing and suction, respectively, and zero value of bleeding coefficient corresponds to impermeable wall.

First, in order to show the effects of bleeding coefficient, σ , on the distribution of Nusselt number along the centerline on the bottom wall, Figure 5 is plotted. This figure shows that the minimum value of Nu occurs adjacent to step corner and then Nu increases sharply in the recirculated region because of the flow vortices. Then Nu reaches to a maximum value at the reattachment point after which the value of Nusselt number decreases and approaches to a constant value as the distance continues to increase in the stream-wise direction. Moreover, Figure 5 shows the effect of bleeding coefficient on the distribution of Nusselt number. This figure shows that suction increases the value of Nu while blowing has opposite effect. This is related to the increased temperature and velocity gradients for the case of suction compared to that of blowing.

Figure 6 presents the distribution of friction coefficient for various values of the bleeding coefficient along the mid-plane on the bottom wall. The coefficient of friction is negative inside the recirculation bubble due to the back flow in this region. At the point of reattachment, the coefficient of friction is zero due to

the vanished velocity gradients. By examining the effect of blowing on coefficient of friction, it is clear that blowing decreases the coefficient of friction, along the permeable wall. This is due to the repulsion of streamlines from the bottom wall by the blowing process. The effect of suction on the coefficient of friction is opposite to that of blowing, such that the value of C_f increases by the suction because of the increased velocity gradient on the permeable wall. It is worth mentioning that after the porous segment area, an opposite trend is seen such that the value of friction coefficient increases in the case of blowing which contradicts with those mentioned before. On this subject, one should recall that in the case of blowing, due to the mass increase, the velocity gradient and consequently the friction coefficient on the bottom wall increases.

In this study, a close attention is paid to the distribution patterns of both the Nusselt number and the skin friction coefficient contours at the bottom wall surface. Figure 7 shows the distribution of Nusselt number contours at the bottom wall surface for different cases of bleeding condition.
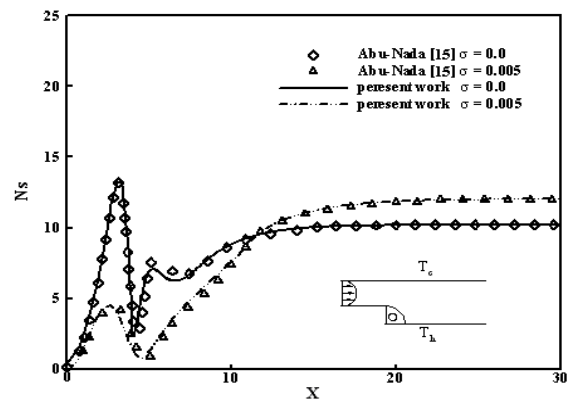

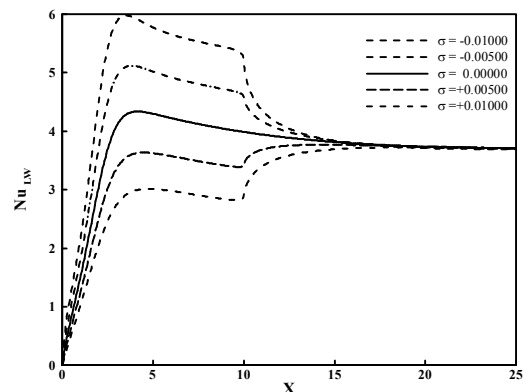**Figure 4.** Distribution of entropy generation on the bottom wall (ER=2).

Figure 5. Nusselt number distribution on the bottom wall along the centerline at deferent values of the bleeding coefficient.
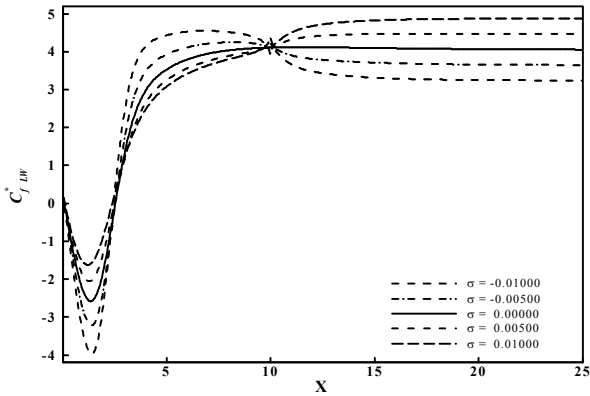
Figure 6. C_f distribution along the centerline on the bottom wall
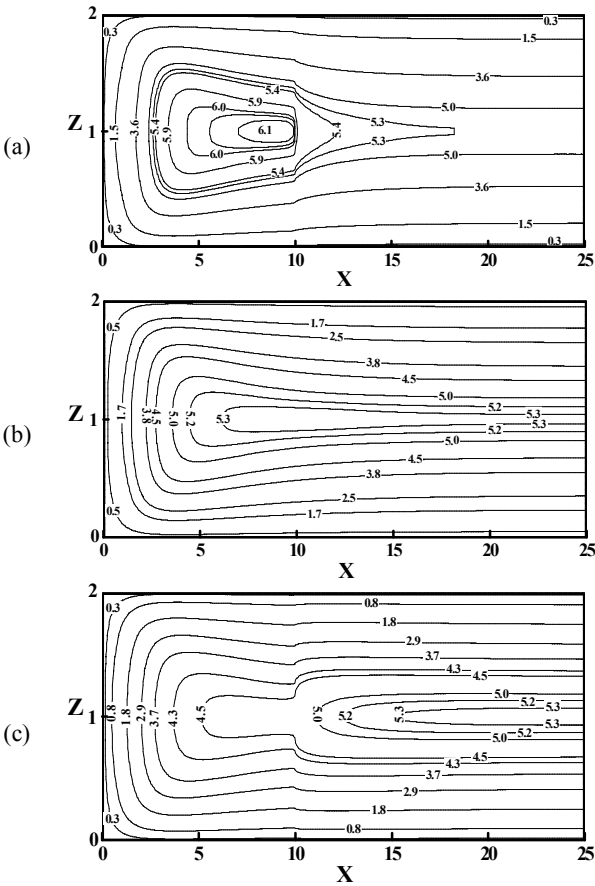

Figure 7. Nusselt number contours on the bottom wall, (a) $\sigma = -0.005$, (b) $\sigma = 0$, (c) $\sigma = 0.005$

Distributions of skin friction coefficient on the bottom wall surface at different values for the bleeding coefficient are shown in Figure 8. As it is seen from this figure, in the case of blowing, the maximum value of friction coefficient occurs just at the centerline of the
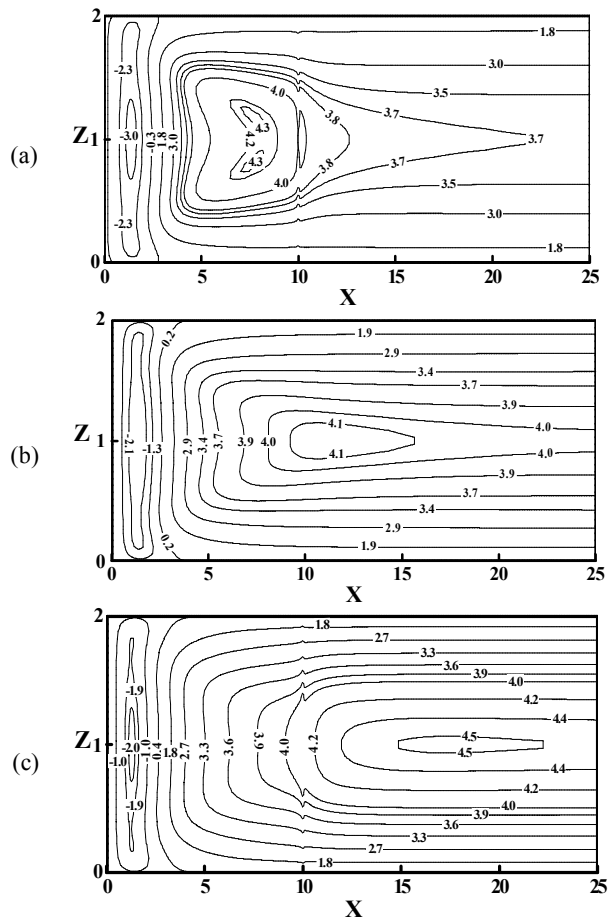

Figure 8. C_f contours on the bottom wall, (a) $\sigma = -0.005$, (b) $\sigma = 0$, (c) $\sigma = 0.005$

bottom wall and shifts to the downstream of the duct, but in the case of suction, $c_{f\,max}$ occurs near the centerline and shifts toward the step. It is also found that the maximum Nusselt number, Nu_{max}, appears near the both side walls, instead of the centerline. It is seen that the location and value of maximum Nusselt number changes with a change in the bleeding coefficient. Besides, Figure 7 reveals that because of the suction process, Nu_{max} shifts toward the upstream direction and its value increases.

Figure 9 shows the distribution of entropy generation number along the centerline on the bottom wall. This figure shows that the minimum value of Ns occurs at the step corner, where the fluid has no motion. As it is seen from this figure, Ns distribution has a local peak which occurs inside the recirculation region, after which Ns increases and approaches to a constant value. In addition, this figure shows the effect of bleeding coefficient on the entropy generation number. It can also be found that suction causes an increase in the value of Ns and blowing has opposite effect.
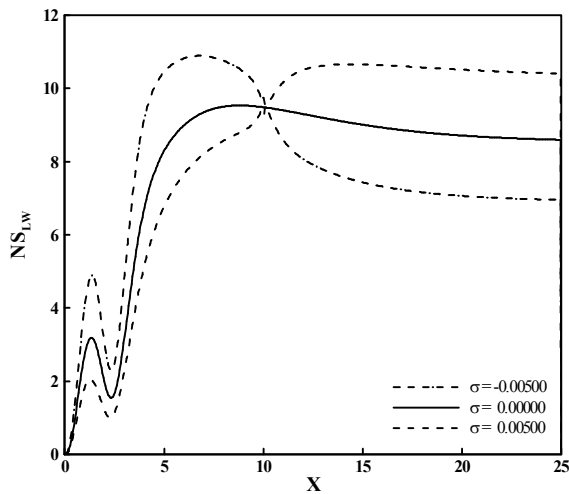
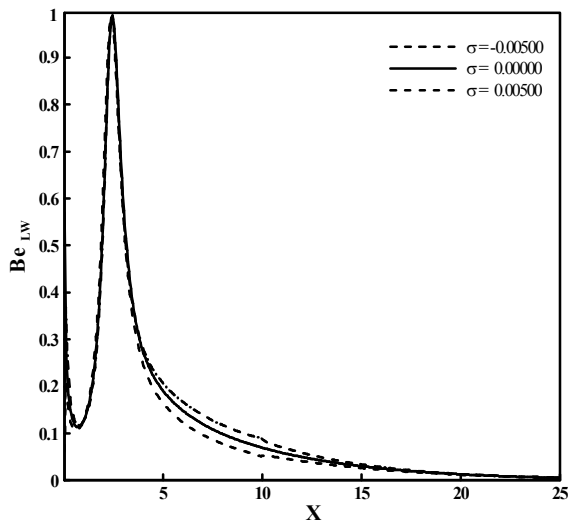**Figure 9.** Variation of Ns along the mid-plane

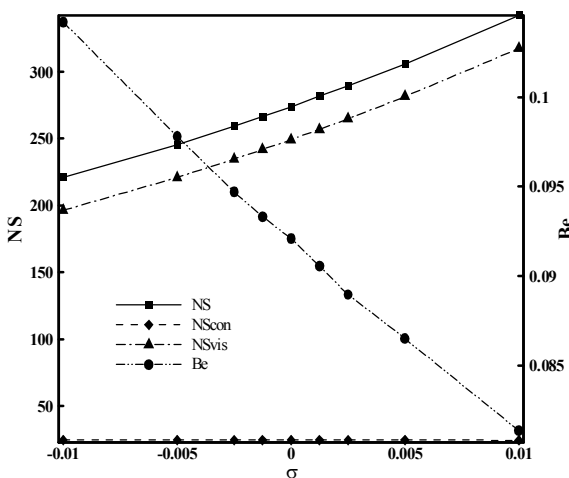**Figure 10.** Bejan number variation along the mid-plane.

Figure 11. Variations of total entropy generation and average Bejan number with bleeding coefficient

This is related to the increased temperature and velocity gradients for the case of suction compared to that of blowing. High values of temperature gradients at the bottom wall results in higher values for entropy generation as it is depicted in Figure 9. Therefore, the enhancement of heat transfer at the bottom wall is accompanied with an increase in the value of Ns. It is worth mentioning that after the porous segment ($10 \leq X \leq 25$), the amount of Ns decreases because of the suction process. As it was mentioned above, in the case of suction, due to the mass reduction, the velocity gradient and consequently the friction coefficient minimizes which causes to a remarkable decrease in the contribution of viscosity entropy generation.

Figure 10 shows the distribution of Bejan number at the bottom wall along the mid-plane. The Bejan number is the ratio of entropy generation due to the conduction to the total entropy generation. It is very clear that at the step corner, where the fluid has no any motion and zero velocity gradient exists, the entropy generation is due to conduction only (Be = 1). Also, the value of Be = 1 occurs at the point of reattachment because the wall shear stress vanishes at this point and the entropy generation is completely due to heat transfer. Also it should be mentioned that because the developing thermal boundaries along the flow direction, the temperature gradient on the bottom wall and consequently, contribution of conductive entropy generation decreases which causes to decrease in the value of Bejan number far from the step.

Figure 11 represents the variation of total entropy generation on the flow domain versus bleeding coefficient. Total entropy generation is an important parameter in convection flow because it shows the amount of irreversibility inside the flow domain. It is seen that blowing increases the value of total entropy generation whereas suction has opposite effect. Also, this figure shows the effect of bleeding coefficient on the average Bejan number. It is seen that the average Bejan number has a decreasing trend by increasing in bleeding coefficient from suction to blowing.

7. CONCLUSION

The present study deals the analysis of entropy generation in three-dimensional laminar forced convection of viscous fluid flow over a backward facing step in a horizontal duct under bleeding condition. The set of governing equations consisting the conservations of mass, momentum, energy and entropy generation is solved numerically by the CFD techniques in the Cartesian coordinate system. The effects of bleeding coefficient on friction coefficient, Nusselt number, entropy generation and Bejan number were investigated. Moreover, total entropy generation which shows the

amount of irreversibility in convection flow is calculated for various bleeding coefficient. It was revealed that the bleeding coefficient has a great effect on the rates of entropy generation and heat transfer in separated convection flow.

8. REFERENCES

1. Armaly, B.F., Li, A. and Nie, J.H., "Measurements in three-dimensional laminar separated flow", *International Journal of Heat and Mass Transfer,* Vol. 46, (2003), 3573–3582.

2. Nie, J.H. and Armaly, B.F., "Reverse flow regions in three-dimensional backward-facing step flow", *International Journal of Heat and Mass Transfer,* Vol. 47, (2004), 4713–4720.

3. Iwai, H., Nakabe, K. and Suzuki, K., "Flow and heat transfer characteristics of backward-facing step laminar flow in a rectangular duct", *International Journal of Heat and Mass Transfer,* Vol. 43 (2000), 457-471.

4. Nie, J.H. and Armaly, B.F., "Three-dimensional convective flow adjacent to backward-facing step - effects of step height", *International Journal of Heat and Mass Transfer*, Vol. 45, (2002), 2431–2438.

5. Nie, J.H. and Armaly, B.F., "Convection in laminar three-dimensional separated flow", *International Journal of Heat and Mass Transfer*, Vol. 47 (2004), 5407–5416.

6. Abu-Mulaweh, H.I., "A review of research on laminar mixed convection flow over backward- and forward facing steps", *International Journal of Thermal Sciences*, Vol. 42 (2003), 897–909.

7. Iwai, H., Nakabe, K., Suzuki, K. and Matsubara, K., "The effects of duct inclination angle on laminar mixed convective flows over a backward-facing step", *International Journal of Heat and Mass Transfer*, Vol. 43, (2000), 473-485.

8. Chen, Y.T., Nie, J.H., Hsieh, H.T. and Sun, L.J., "Three-dimensional convection flow adjacent to inclined backward-facing step", *International Journal of Heat and Mass Transfer*, Vol. 49, (2006), 4795–4803.

9. Nie, J.H., Chen, Y.T. and Hsieh, H.T., "Effects of a baffle on separated convection flow adjacent to backward-facing step", *International Journal of Thermal Sciences*, Vol. 48, (2009), 618–625.

10. Bejan, A., "A study of entropy generation in fundamental convective heat transfer", *Journal of Heat Transfer*, Vol. 101, (1979), 718–725.

11. Bejan, A., "The thermodynamic design of heat and mass transfer processes and devices", *Journal of Heat and Fluid Flow*, Vol. 8, (1987), 258-275.

12. Drost M. K. and White, M. D., "Numerical prediction of local entropy generation in an impinging jet", *Journal of Heat Transfer*, Vol. 113, (1991), 823-829.

13. Abu-Nada, E., "Numerical prediction of entropy generation in separated flows", *Entropy*, Vol. 7, (2005), 234–252.

14. Abu-Nada, E., "Entropy generation due to heat and fluid flow in backward facing step flow with various expansion ratios", *International Journal of Energy*, Vol. 3, (2006), 419–435.

15. Abu-Nada, E., "Investigation of entropy generation over a backward facing step under bleeding conditions", *Energy Conversion and Management*, Vol. 49, (2008), 3237–3242.

16. Bahrami A. and Gandjalikhan Nassab, S. A., "Study of Entropy Generation in Laminar Forced Convection Flow over a Forward-Facing Step in a Duct", *International Review of Mechanical Engineering*, Vol. 4, No. 4, (2010), 399-404.

17. Atashafrooz, M., Gandjalikhan Nassab, S. A. and Ansari, A. B., "Numerical study of entropy generation in laminar forced convection flow over inclined backward and forward facing steps in a duct", *International Review of Mechanical Engineering*, in press, 2011.

18. Patankar, S. V. and Spalding, D. B., "A calculation procedure for heat, mass and momentum transfer in three-dimensional parabolic flows", *International Journal of Heat and Mass Transfer*, Vol. 15, No. 10, (1972), 1787–1806.

19. Li, A., "Experimental and numerical study of three-dimensional laminar separated flow adjacent to backward-facing step", Ph.D. thesis, University of Missouri, Rolla, MO, 2001.

20. Bejan, A., "Entropy Generation through Heat and Fluid Flow", Wiley Interscience, New York, 1982.

Ivestigation of Entropy Generation in 3-D Laminar Forced Convection Flow over a Backward Facing Step with Bleeding

M. Shamsi Kooshki[a], S. A. Gandjalikhan Nassab [a] , A. B. Ansari[b]

[a] Department of Mechanical Engineering, Shahid Bahonar University, kerman, Iran
[b] Department of Mechanical Engineering, Tehran University, Tehran, Iran

---

چکیده

کار حاضر به مطالعه عددی تولید انتروپی در جریان جابجایی آرام گاز از روی پله پسرو در داخل کانال همراه با مکش و دمش پرداخته است. به منظور محاسبه شدت تولید انتروپی با استفاده از قانون دوم، تعیین میدان سرعت و دما مورد نیاز است. در این راستا با بکارگیری مختصات کارتزین، معادلات حاکم شامل بقای جرم، ممتم و انرژی با تکنیک دینامیک سیالات محاسباتی حل عددی شده اند. فرم مجزای این معادلات با روش حجم محدود بدست آمده و توسط آلگوریتم سیمپل به جواب رسیده اند. با داشتن نتایج عددی، تاثیر عمل دمش و مکش بر توزیع شدت تولید انتروپی روی دیواره های کانال و همچنین بر روی کل تولید انتروپی در داخل جریان مورد مطالعه قرار گرفته است. نتایج حاضر می توانند در راستای طراحی سیستمهای حرارتی با بازدهی بالا مفید باشند. مقایسه نتایج عددی بدست آمده با داده های موجود در مراجع معتبر سازگاری خوبی را نشان می دهد.